

PAPER

Vertical $\beta\text{-Ga}_2\text{O}_3$ Schottky rectifiers with 750 V reverse breakdown voltage at 600 K

To cite this article: Xinyi Xia *et al* 2021 *J. Phys. D: Appl. Phys.* **54** 305103

View the [article online](#) for updates and enhancements.






IOP | ebooks™

Bringing together innovative digital publishing with leading authors from the global scientific community.

Start exploring the collection—download the first chapter of every title for free.

Vertical β -Ga₂O₃ Schottky rectifiers with 750 V reverse breakdown voltage at 600 K

Xinyi Xia¹, Minghan Xian¹, Patrick Carey¹, Chaker Fares¹, Fan Ren¹, Marko Tadjer² , S J Pearton^{3,*} , Thieu Quang Tu⁴, Ken Goto⁵  and Akito Kuramata⁴

¹ Department of Chemical Engineering, University of Florida, Gainesville, FL 32611, United States of America

² Naval Research Laboratory, Washington, DC 20375, United States of America

³ Department of Materials Science and Engineering, University of Florida, Gainesville, FL 32611, United States of America

⁴ Novel Crystal Technology, Inc, Saitama, Sayama-Shi, Japan

⁵ Department of Applied Chemistry, Tokyo University of Agriculture and Technology, Koganei, Tokyo 184-8588, Japan

E-mail: spear@mse.ufl.edu

Received 14 March 2021, revised 5 April 2021

Accepted for publication 5 May 2021

Published 18 May 2021



Abstract

Field-plated vertical Ga₂O₃ rectifiers were operated up to 600 K with reverse breakdown voltage (V_B) of 750 V, 950 V at 500 K and 1460 V at 400 K. The barrier height was 1.3 eV at 300 K and reduced to 0.7 eV at 600 K, with ideality factors of 1.05 ± 0.05 and 2 ± 0.1 , respectively at these temperatures. On-state resistance, R_{ON} , was $13 \text{ m}\Omega \text{ cm}^2$ at 300 K and $41 \text{ m}\Omega \text{ cm}^2$ at 600 K, leading to respective Baliga figures of merit of 151 MW cm^{-2} (300 K) and 13.9 MW cm^{-2} (600 K). The on-off ratio was $>10^4$ for all temperatures measured. The leakage current showed a good fit to the thermionic field emission model when the reverse voltage was less than 80 V, and it was dominated by the tunneling effect at higher voltage. The transition voltage from thermionic emission to tunneling effect decreased as the temperature increased. At high reverse voltage, a large number of electrons are injected into the drift region, and the current shows an $I \propto V^n$ relationship with voltage, indicating a trap-assisted space-charge-limited conduction (SCLC) mechanism. We observed this SCLC relation when the reverse voltage was larger than 400 V for 500 and 600 K. The associated trap energies for these two regions were extracted as 0.2 and 0.4 eV, consistent with levels in the gap.

Keywords: Ga₂O₃, rectifier, power electronics

(Some figures may appear in colour only in the online journal)

1. Introduction

The development of power electronics technology based on wide bandgap semiconductors is attracting much interest because of the potential for significantly higher switching efficiency and ability to operate at higher powers and temperatures. Within the next decade, about 80% of all US electricity

is expected to flow through power electronics. These include power distribution systems, electric vehicle fast chargers, data center power supplies, ship power systems, and renewable wind/solar energy integration. Both SiC and GaN power electronics are now commercialized and provide more efficient performance than conventional Si-based devices [1–3]. The combination of high breakdown voltage, low on-state resistance and lower switching losses is improved in the ultra-wide bandgap semiconductors [4–10] (such as Ga₂O₃,

* Author to whom any correspondence should be addressed.

diamond, and AlN). This leads to their high Baliga's figure of merit (BFOM), defined as $\varepsilon \cdot \mu \cdot E_c^3$, where ε , μ , and E_c are the dielectric constant, carrier mobility, and critical breakdown field strength, respectively.

Among these ultra-wide bandgap semiconductors, monoclinic gallium oxide (β -Ga₂O₃) has recently attracted increasing attention due to the availability of high quality, large diameter single crystals from mature melt growth methods and its attractive material properties of wide E_G of 4.6–4.9 eV, good electron mobility ($>200 \text{ cm}^2 \text{ V}^{-1} \text{ s}^{-1}$) and estimated critical breakdown field, E_c , of $\sim 8 \text{ MV cm}^{-1}$, yielding a relatively high BFOM (>3000) with respect to silicon [11–23]. Compared to other ultra-wide bandgap materials, the inexpensive substrates lower the manufacturing cost for β -Ga₂O₃ power devices for applications requiring high operation voltage and high energy conversion efficiency.

A large literature on demonstration of power devices in this materials system now exists, including vertical and lateral MOSFETs and rectifiers [6–41]. The absence of practical p-type doping may be alleviated by use of other p-type oxide semiconductors to form a pn heterojunction with Ga₂O₃, such as NiO, Cu₂O, CuI and Ir₂O₃ [26–32]. Some notable recent advancements in device performance for Ga₂O₃ diodes includes a 5 A/700 V junction Schottky barrier diode implemented with p-type NiO layer [33], 1.86 kV p–n junction diode with NiO heterojunction [34], as well as demonstrations of $>100 \text{ A}$ of absolute forward current using conventional field-plated Schottky diodes [35].

Wide energy bandgap materials are suitable for high temperature as well as high breakdown voltage applications. The ability to operate at high temperature enables wide bandgap devices to be attractive in terms of reduced package size and minimal requirement for cooling. Hindered by its low thermal conductivity, demonstrations of operation at high temperature for β -Ga₂O₃ are fairly limited. Wang *et al* [36] reported operation up to 600 K of rectifiers with beveled edge termination and spin-on glass passivation, achieving breakdown voltage of $\sim 500 \text{ V}$ at this temperature. One way to increase the breakdown voltage is to grow thicker layers, but to date, the maximum drift layer thickness has been $30 \mu\text{m}$, thinned to $20 \mu\text{m}$ after the chemical mechanical planarization (CMP) step needed to achieve a flat surface morphology [15].

In this work, we report operation of field plated Schottky barrier diodes up to 750 V at 600 K, with reasonable leakage current density. This was achieved by growing a $40 \mu\text{m}$ thick drift layer, thinned to $30 \mu\text{m}$ after CMP, as well as lower carrier concentration. The devices exhibit a negative temperature coefficient of breakdown and reverse leakage dominated by thermionic field emission (TFE) when the reverse voltage was less than 80 V, and by tunneling conduction at higher voltage.

2. Experimental

The drift region of the material consisted of a $30 \mu\text{m}$ thick, lightly Si doped epitaxial layer grown by halide vapor phase epitaxy (HVPE) with minimum carrier concentration of $1.6 \times 10^{16} \text{ cm}^{-3}$ (the maximum was $\sim 3 \times 10^{16} \text{ cm}^{-3}$), and

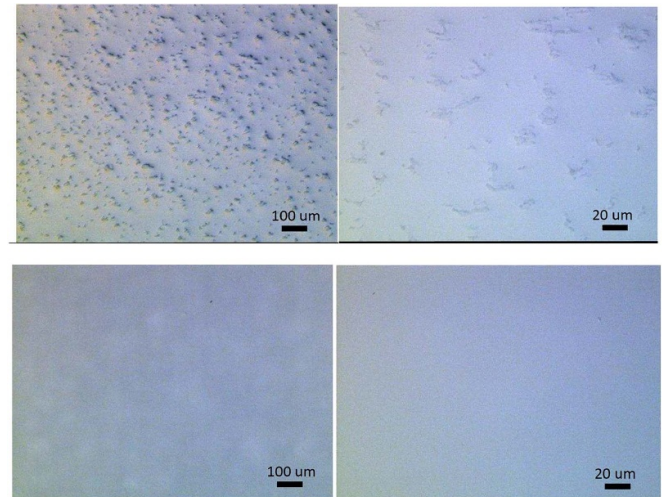


Figure 1. Nomarski microscope images of the HVPE layers before (top, left and right) and after subsequent polishing to planarize the surface (bottom, left and right).

this epitaxial layer was grown on a (001) surface orientation Sn-doped β -Ga₂O₃ single crystal (Novel Crystal Technology, Japan). The HVPE layer is actually grown initially to a thickness of $\sim 40 \mu\text{m}$, but then chemically mechanically polished to planarize the surface by removing $\sim 10 \mu\text{m}$ of material. As seen in the Nomarski images of figure 1, this produces a much smoother surface relative to the as-grown morphology, but there is still some surface roughness after the CMP step. It is important to note that this is a unique growth, the thickest ever attempted at NCT and the process is not optimized.

A full area Ti/Au backside Ohmic contact was formed by e-beam evaporation and was annealed at 550 C for 30 s under N₂ ambient. 40 nm of Al₂O₃ and 400 nm of SiN_x were deposited as field plate dielectric using Cambridge-Nano-Fiji ALD and PlasmaTherm PECVD tools. Dielectric windows of $40 \times 40 \mu\text{m}$ was opened using dilute buffered oxide etchant (BOE), and a 200 nm Ni/Au Schottky contact was deposited with E-beam after lithography pattern followed by standard acetone lift-off. Figure 2 shows a photograph and device geometry of fabricated diodes, respectively. Of the 121 devices on this chip, approximately 46 have very smooth morphology, but this was not the only parameter that correlated with achieving high breakdown voltage. We had a yield of $\sim 15\%$ (~ 20 devices out of 121) with breakdown in the range 745–754 V. The carrier concentration of these highest breakdown voltages was typically $<2 \times 10^{16} \text{ cm}^{-3}$ with no visible surface defects within the active area of the device. The remaining surface defects are due to the incomplete smoothing of the surface of the HVPE-grown layer.

The current–voltage (I – V) characteristics were recorded at 1 MHz with a Tektronix 370 A curve tracer was used for forward and reverse current measurements over the temperature range 300–600 K on a temperature-controlled stage. No hysteresis was observed in any of the rectifier characteristics. The forward direction was dominated by the thermionic emission (TE) current, while in the reverse direction, the TFE

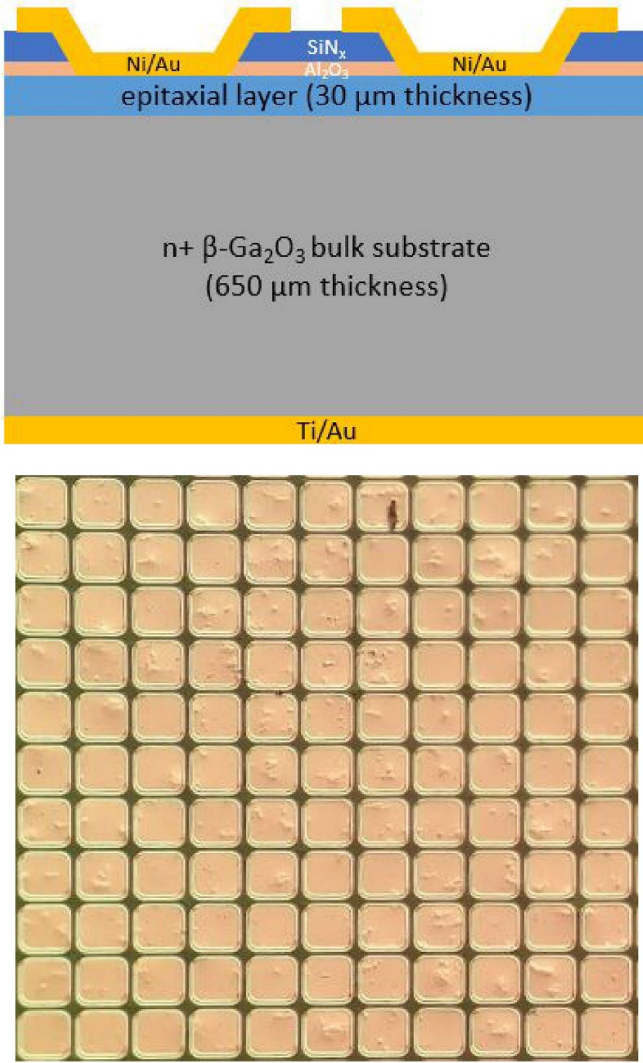


Figure 2. Schematic of vertical rectifier structure (top) and photograph of fabricated β -Ga₂O₃ Schottky diode array with $40 \times 40 \mu\text{m}$ squares (bottom).

and tunneling currents played an important role at high reverse bias. To extract the barrier height (Φ_b) and ideality factor (n), we used the relationship for current density in TE theory, given by [1, 3, 36]

$$J = J_0 \exp(eV_A/nkT) [1 - \exp(-eV_A/kT)]$$

where $J_0 = A^* m_{\text{eff}}/m_0 T^2 \exp(\Phi_B/kT)$, e is electronic charge and A^* is the Richardson constant and V_A is the bias voltage applied. The magnitude of the series resistance can also be obtained from plots of $d(V_A)/d(\ln J)$ versus J , while the barrier height is obtained from $(kT/e) \ln(A^* T^2/J_0)$ [42, 43]. The built-in voltage can be obtained from the C - V characteristics [43]. The fact that TFE was the dominant current transport mechanism over most of the conditions investigated can be established by the fact that the tunneling parameter E_{00}/kT was ~ 1 [40], where E_{00} is given by $(eh/4\pi)[N_D/m^* \epsilon_r]^{0.5}$ and h is Planck's constant and ϵ_r is the relative dielectric constant. If this parameter is much less than unity, then TE is significant and field emission is dominant if this parameter is $\gg 1$.

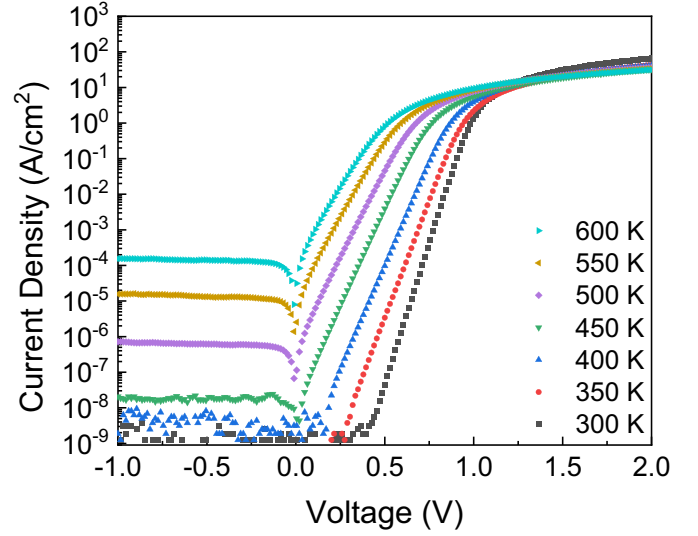


Figure 3. Forward I - V characteristic for rectifiers as a function of temperature.

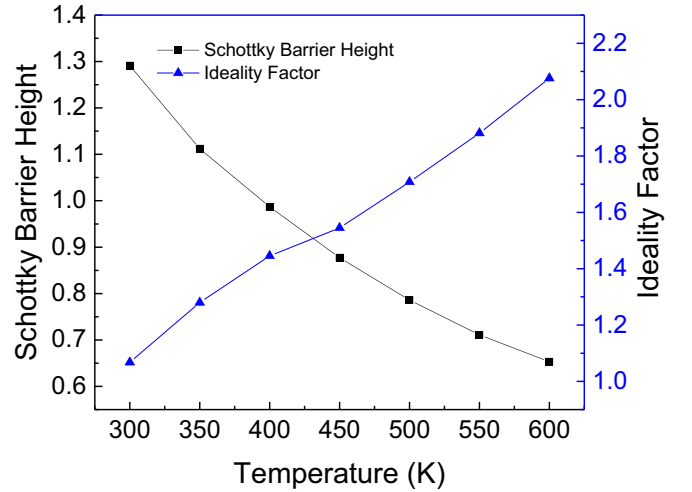


Figure 4. Schottky barrier height and ideality factor retrieved from diode forward I - V as a function of temperature.

Capacitance–voltage (C - V) characteristics were recorded with an Agilent 4284 A Precision LCR Meter. The diode on/off ratio is another figure-of-merit was measured when switching from 2 V forward to reverse biases up to 100 V. The reverse breakdown voltage was defined as the bias for a reverse current of 1 mA.

3. Results and Discussion

The barrier height was 1.23 eV at 300 K and reduced to 0.7 eV at 600 K, with ideality factors of 1.05 ± 0.5 and 2 ± 0.1 , respectively at these temperatures, extracted from the I - V - T characteristics in figure 3 and those parameters plotted in figure 4. It is commonly observed that the barrier height decreases with increasing temperature, as it is easier for electrons to pass over the barrier since with pure TE there would be a reduced barrier at elevated temperatures. This will

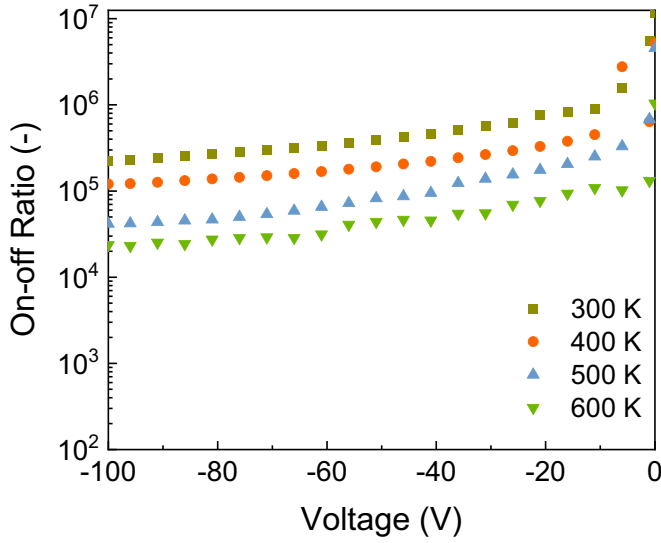


Figure 5. On/off ratio when switching from 2 V forward bias to the reverse biases shown on the x -axes at various temperatures.

lead to contributions from other transport mechanisms and the commonly observed higher ideality factors at elevated temperatures [40]. There may also be contributions from spatial inhomogeneity of the Schottky barrier [40].

The temperature coefficient was $-(2.1 \pm 0.6) \times 10^{-3} \text{ eV K}^{-1}$, which is the same order of magnitude as the temperature dependence of the band gap, namely $(-4.5 \times 10^{-3}) \text{ eV K}^{-1}$ [38]. In Si, the temperature coefficient of the barrier height also depends on the chemical nature of the metal, in contradiction with models suggesting Fermi-level pinning at the center of the semiconductor's band gap [39]. In Ga_2O_3 , the situation is more complex, with the dependence of barrier height on metal work function being a function of the orientation of the Ga_2O_3 surface. It is generally the case that a number of factors also have an influence on barrier height and its temperature dependence. For Ga_2O_3 , these factors include the interface crystallography, contact inhomogeneities, the recombination velocities on different surface planes of Ga_2O_3 or for different polytypes. For example, Lyle *et al* [40] found a strong positive correlation between the calculated Schottky barrier heights and the work function of metal contacts on (100) $\beta\text{-Ga}_2\text{O}_3$, in contrast to (201) $\beta\text{-Ga}_2\text{O}_3$. Similarly, there were mixed results for (010) $\beta\text{-Ga}_2\text{O}_3$ [40]. The temperature dependence of barrier height and ideality factor in our devices is consistent with previous reports [36, 41]. We did not observe any significant change in carrier concentration as a result of the temperature cycling, as judged from the C - V measurements.

The on-state resistance of the rectifiers, R_{ON} , was $13 \text{ m}\Omega \text{ cm}^2$ at 300 K and $41 \text{ m}\Omega \text{ cm}^2$ at 600 K, leading to respective Baliga figures of merit of 150 MW cm^{-2} (300 K) and 14 MW cm^{-2} (600 K). The highest previous result was 4 MW cm^{-2} at 600 K [36]. The series resistance of the highest breakdown voltage rectifiers was typically between 200 and 300Ω . The on-off ratio is another figure of merit in that having high on-current and low leakage current in reverse bias is desirable [44–47]. This was $>10^4$ for all temperatures measured, as shown in figure 5.

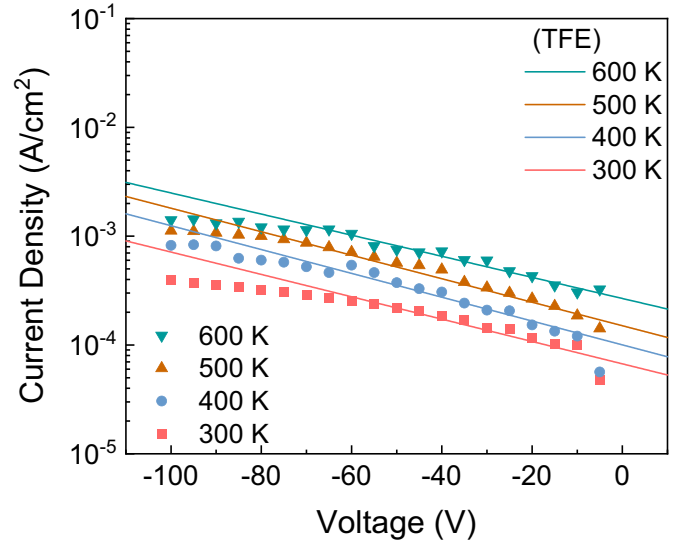


Figure 6. Reverse current density of the vertical $\beta\text{-Ga}_2\text{O}_3$ Schottky diode at various temperatures fitted to the TFE model for reverse biases of 5–100 V.

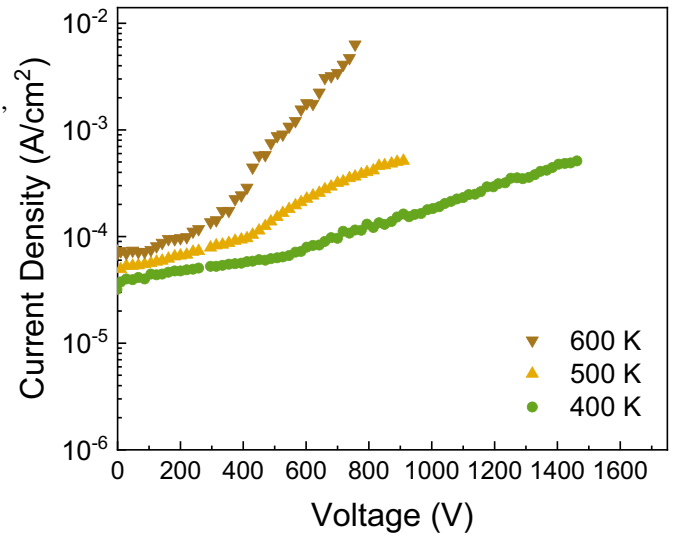


Figure 7. Reverse I - V - T characteristics at 400–600 K for rectifiers at various temperatures.

As shown in figure 6, at lower voltages, reverse bias leakage current is dominated by TFE [36, 37], which is dependent on ambient temperature. However, with increasing voltage and hence electric field, the carrier tunneling and other conduction processes becomes predominant, and the leakage currents become more sensitive to temperature changes [48]. The leakage current shows a good fit to the TFE model when the reverse voltage is less than 80 V in figure 6, and it is affected by the tunneling effect when voltage is higher than 80 V. However, the transition voltage from TE to tunneling effect did not follow the universal monotonic temperature [36, 37]. The transition voltage actually decreased as the temperature increased, as illustrated in figure 7, showing that impact ionization is not the breakdown mechanism, since that should exhibit positive

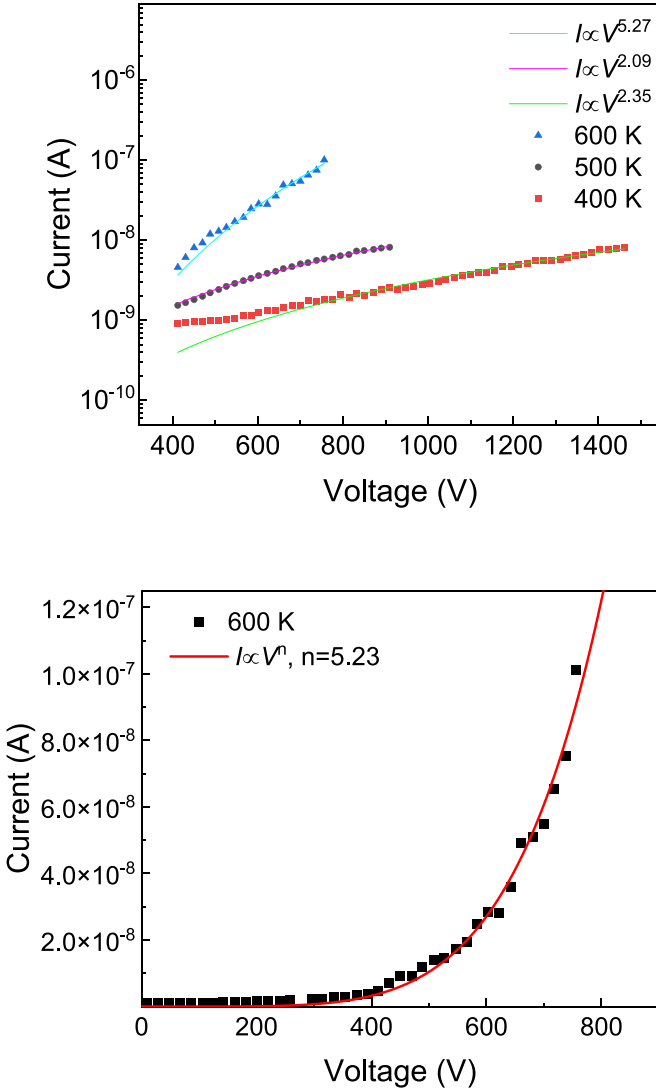


Figure 8. Experimental data for reverse current characteristics at 400–600 K and fit to an $I \propto V^n$ relationship (top) and more detailed view of 600 K reverse current characteristic and fit to an $I \propto V^n$ relationship with $n = 5.2$ (bottom).

temperature coefficient [44]. The variation of V_B with temperature can be represented by a relation of the form [45]:

$$V_B = V_{B0} [1 + \beta(T - T_0)]$$

where $\beta = -3.4 \pm 1.4 \text{ V K}^{-1}$. We have previously found that current increases in vertical geometry Ga_2O_3 rectifiers during electron beam induced current measurements are dominated by impact ionization of deep acceptors in the depletion region. At room temperature, mobile hole diffusion in the quasi-neutral region of Schottky diodes contributes significantly to the charge collection efficiency [46]. Electron beam induced current measurements indicated a strong amplification of photocurrent in rectifiers, attributed to the Schottky barrier lowering by holes trapped on acceptors near the surface [47].

The breakdown fields calculated from the observed breakdown voltages at different temperatures were

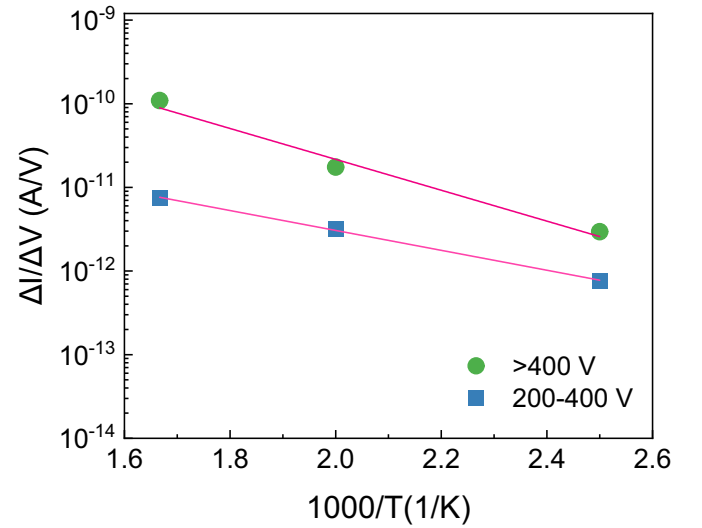


Figure 9. Arrhenius plot $\Delta I / \Delta V$ versus $1/T$. The I – V slope of the voltages ranges from 200 to 400 V, and ranges over 400 V for rectifiers measured as a function of temperature.

$5.0 \times 10^5 \text{ V cm}^{-1}$ at 600 K, $6.3 \times 10^5 \text{ V cm}^{-1}$ at 500 K and $9.8 \times 10^5 \text{ V cm}^{-1}$ at 400 K. These were obtained from the non-punch through relation $E_{bd} = [(2eN_d V_{bd})/\epsilon]^{0.5}$ [48]. Currently, all Ga_2O_3 rectifiers show performance limited by the presence of defects and by breakdown initiated in the depletion region near the electrode corners.

When a higher reverse voltage is applied, a large number of electrons are injected into the drift region, and the current shows an $I \propto V^n$ relationship with the voltage, indicating a trap-assisted space-charge-limited conduction (SCLC) mechanism [49, 50]. Under this mechanism, a current hump should be observed before the trap-filled limited voltage, and with electrons continue to be injected into the drift region, it will lead to a breakdown. This is commonly reported in GaN, i.e. the logarithmic I – V curve shows that the current I is proportional to V^n until a hump (sharp transition in I – V curve) at some threshold voltage. Such behavior can be modeled by a space-charge-limited current (SCLC) conduction mechanism with traps [51, 52]. Under reverse bias and below this threshold, electrons injected into the drift layer partly contribute to conduction current and are partly captured by acceptor traps known to be present. The hump threshold voltage represents the trap-filled-limited voltage of the acceptor traps, suggesting the applied voltage overcomes the negative potential formed by the un-neutralized electrons in traps and the ionized donors in the n- Ga_2O_3 [51, 52]. This shows an SCLC relation when the reverse voltage is larger than 400 V for 500 and 600 K in figure 7.

The reverse current characteristics at different temperatures are shown in more detail in figure 8 (top), with all showing $I \propto V^n$ relationship. A fit to the data for the 600 K reverse current characteristic is shown at the bottom of figure 8. The data fits well to a relationship $I \propto V^n$, where n is 5.2 and the constant of proportionality is 7.6×10^{-23} . The associated trap energies for these two regions were extracted as 0.2 and 0.4 eV from an Arrhenius plot, as shown in figure 9. Levels

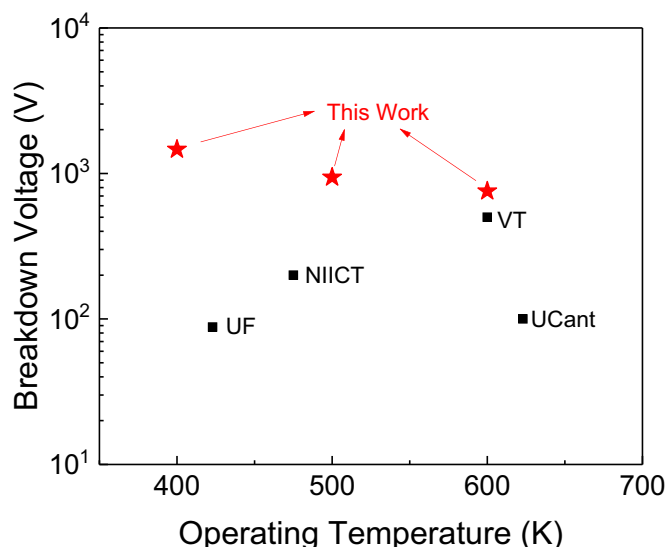


Figure 10. Comparison of operation temperature versus maximum reverse bias for reported vertical Ga_2O_3 rectifiers. Previous data comes from Virginia Tech [36], University of Canterbury [54], University of Florida [55] and NIICT [56].

with these activation energies have been reported previously in epitaxial Ga_2O_3 , but were ascribed to unknown impurities and native point defects, respectively, with no specific information on their microstructure [53].

The record high reverse breakdown at high temperature in this work is a significant advance for high temperature switching applications for $\beta\text{-Ga}_2\text{O}_3$, as shown in the reverse breakdown performance when compared with previous reported works at elevated temperature in figure 10.

4. Summary and conclusions

Ultrawide bandgap semiconductors offer higher switching frequencies, higher operating temperatures and lower losses that improve power conversion efficiency. The remaining challenges and new opportunities for Ga_2O_3 in high power applications ranging from electric vehicles, medium voltage motor drives, renewable energy interfaces, microgrids, to emerging applications such as electric propulsion for aircraft include more thermally stable contacts, development of stable MOS gates, optimized edge termination and continued improvements in epi and bulk growth. For EV motor drives, the improved efficiency of ultra wide bandgap semiconductor devices would enable either extended range for the vehicle for a given battery charge, or a reduction in the battery pack required to go a certain distance. The required power modules would need large area MOSFETs delivering current in the range of 80–120 Amps per chip at 650 to 1200 V. The promising results from vertical Ga_2O_3 rectifiers reported previously in terms of breakdown voltages and now high temperature operation suggest that thermal management issues become more important to address.

Data availability statement

All data that support the findings of this study are included within the article (and any supplementary files).

Acknowledgments

The work at UF was performed as part of Interaction of Ionizing Radiation with Matter University Research Alliance (IIRM-URA), sponsored by the Department of the Defense, Defense Threat Reduction Agency under award HDTRA1-20-2-0002. The content of the information does not necessarily reflect the position or the policy of the federal government, and no official endorsement should be inferred. The work at UF was also supported by NSF DMR 1856662 (James Edgar). The work at NRL was supported by the Office of Naval Research.

ORCID iDs

Marko Tadjer  <https://orcid.org/0000-0002-2388-2937>

S J Pearton  <https://orcid.org/0000-0001-6498-1256>

Ken Goto  <https://orcid.org/0000-0002-3371-0020>

References

- [1] Millán J, Godignon P, Perpiñà X, Tomás A P and Rebollo J 2014 A survey of wide bandgap power semiconductor devices *IEEE Trans. Power Electron.* **29** 2155
- [2] Zhao Y and Palacios T 2020 Ultra wide bandgap vertical power FinFETs *IEEE Trans. Electron Dev.* **67** 3960
- [3] Huang A Q 2017 Power semiconductor devices for smart grid and renewable energy systems *Proc. IEEE* **105** 2019
- [4] Higashiwaki M, Sasaki K, Murakami H, Kumagai Y, Koukita A, Kuramata A, Takekazu M and Yamakoshi S 2016 Recent progress in Ga_2O_3 power devices *Semicond. Sci. Technol.* **31** 034001
- [5] Fujita S 2015 Wide-bandgap semiconductor materials: for their full bloom *Japan. J. Appl. Phys.* **54** 030101
- [6] Pearton S J, Yang J, Cary P H, Ren F, Kim J, Tadjer M J and Mastro M A 2018 A review of Ga_2O_3 materials, processing, and devices *Appl. Phys. Rev.* **5** 011301
- [7] Allen N, Xiao M, Yan X, Kohei Sasaki M J, Tadjer J M, Zhang R, Wang H and Zhang Y 2019 Vertical Ga_2O_3 schottky barrier diodes with small-angle beveled field plates: a baliga's figure-of-merit of 0.6 GW/cm^2 *IEEE Electron Dev. Lett.* **40** 1399
- [8] Konishi K, Goto K, Murakami H, Kumagai Y, Kuramata A, Yamakoshi S and Higashiwaki M 2017 1-kV vertical Ga_2O_3 field-plated Schottky barrier diodes *Appl. Phys. Lett.* **110** 103506
- [9] Pearton S J, Ren F, Tadjer M and Kim J 2018 Perspective: Ga_2O_3 for ultra-high power rectifiers and MOSFETs *J. Appl. Phys.* **124** 220901
- [10] Bader S J et al 2020 Prospects for wide bandgap and ultrawide bandgap CMOS devices *IEEE Trans. Electron Dev.* **67** 4010
- [11] Hu Z et al 2018 Field-plated lateral $\beta\text{-Ga}_2\text{O}_3$ Schottky barrier diode with high reverse blocking voltage of more than 3 kV and high DC power figure-of-merit of 500 MW/cm^2 *IEEE Electron Dev. Lett.* **39** 1564
- [12] Li W, Nomoto K, Hu Z, Jena D and Xing H G 2020 Field-plated Ga_2O_3 trench schottky barrier diodes with a

- BV²/Ron of up to 0.95 GW/cm² *IEEE Electron Dev. Lett.* **41** 107
- [13] Li W, Nomoto K, Hu Z, Nakamura T, Jena D and Xing H G 2019 Single and multi-fin normally-off Ga₂O₃ vertical transistors with a breakdown voltage over 2.6 kV 2019 *IEEE Int. Electron Devices Meeting (IEDM)* p 12.4.1–4
 - [14] Ji M, Taylor N R, Kravchenko I, Joshi P, Tolga Aytug L R and Parans Paranthaman C M 2021 Demonstration of large-size vertical Ga₂O₃ Schottky barrier diodes *IEEE Trans. Power Electron.* **36** 41
 - [15] Yang J C, Ren F, Tadjer M J, Pearton S J and Kuramata A 2018 2300V reverse breakdown voltage Ga₂O₃ Schottky rectifiers *ECS J. Solid State Sci. Technol.* **7** Q92
 - [16] Yang J, Ren F, Chen Y T, Liao Y T, Chang C W, Lin J, Tadjer M J, Pearton S J and Kuramata A 2019 Dynamic switching characteristics of 1 A forward current Ga₂O₃ rectifiers *J. Electron. Dev. Soc.* **7** 57
 - [17] Gao Y et al 2019 High-voltage β -Ga₂O₃ Schottky diode with argon-implanted edge termination *Nanoscale Res. Lett.* **14** 8
 - [18] Hu Z et al 2020 Beveled fluoride plasma treatment for vertical -Ga₂O₃ Schottky barrier diode with high reverse blocking voltage and low turn on voltage *IEEE Electron Dev. Lett.* **4** 441
 - [19] Yang J et al 2019 Vertical geometry 33.2 A, 4.8 MW cm² Ga₂O₃ field-plated Schottky rectifier arrays *Appl. Phys. Lett.* **114** 232106
 - [20] Buttay C, Wong H-Y, Wang B, Xiao M, DiMarino C and Zhang Y 2020 Surge current capability of ultra-wide-bandgap Ga₂O₃ schottky diodes *Microelectron. Reliab.* **114** 113743
 - [21] Zhang H, Yuan L, Tang X, Jichao H, Sun J, Zhang Y, Zhang Y and Jia R 2020 Progress of ultra-wide bandgap Ga₂O₃ semiconductor materials in power MOSFETs *IEEE Trans. Power Electron.* **35** 5157
 - [22] Xiao M et al 2021 Packaged Ga₂O₃ schottky rectifiers with over 60 A surge current capability *IEEE Power Electron. Lett.* (<https://doi.org/10.1109/TPEL.2021.3049966>)
 - [23] Sasaki K, Wakimoto D, Thieu Q T, Koishikawa Y, Kuramata A, Higashiwaki M and Yamakoshi S 2017 First demonstration of Ga₂O₃ trench MOS-type Schottky barrier diodes *IEEE Electron Dev. Lett.* **38** 783
 - [24] He Q and Wenxiang M 2018 Schottky barrier rectifier based on (100) β -Ga₂O₃ and its DC and AC characteristics *IEEE Electron Dev. Lett.* **39** 556
 - [25] Zhou H, Si M, Alghamdi S, Qiu G, Yang L and Ye P D 2017 High- performance depletion/enhancement-ode β -Ga₂O₃ on insulator (GOOI) field-effect transistors with record drain currents of 600/450 mA/mm *IEEE Electron Dev. Lett.* **38** 103
 - [26] Watahiki T, Yuda Y, Furukawa A, Yamamuka M, Takiguchi Y and Miyajima S 2017 Heterojunction p-Cu₂O/n-Ga₂O₃ diode with high breakdown voltage *Appl. Phys. Lett.* **111** 222104
 - [27] Hao W, Qiming H, Zhou K, Guangwei X, Xiong W, Zhou X, Jian G, Chen C, Zhao X and Long S 2021 Low defect density and small curve hysteresis in NiO/ β -Ga₂O₃ pn diode with a high PFOM of 0.65 GW/cm² *Appl. Phys. Lett.* **118** 043501
 - [28] Kokubun Y, Kubo S and Nakagomi S 2016 All-oxide p-n heterojunction diodes comprising p-type NiO and n-type β -Ga₂O₃ *Appl. Phys. Express* **9** 091101
 - [29] Kan S-I, Takemoto S, Kaneko K, Takahashi I, Sugimoto M, Shinohe T and Fujita S 2018 Electrical properties of α -Ir₂O₃/ α -Ga₂O₃ pn heterojunction diode and band alignment of the heterostructure *Appl. Phys. Lett.* **113** 212104
 - [30] Gallagher J C, Koehler A D, Tadjer M J, Mahadik N A, Anderson T J, Budhathoki S, Law K-M, Hauser A J, Hobart K D and Kub F J 2019 Demonstration of CuI as a P-N heterojunction to β -Ga₂O₃ *Appl. Phys. Express* **12** 104005
 - [31] Ghosh S, Baral M, Kamparath R, Choudhary R J, Phase D M, Singh S D and Ganguli T 2019 Epitaxial growth and interface band alignment studies of all oxide α -Cr₂O₃/ β -Ga₂O₃ p-n heterojunction *Appl. Phys. Lett.* **115** 061602
 - [32] Lu X, Zhou X, Jiang H, Ng K W, Chen Z, Pei Y, Lau K M and Wang G 2020 1-kV Sputtered p-NiO/n-Ga₂O₃ heterojunction diodes with an ultra-low leakage current below 1 μ A/cm² *IEEE Electron Dev. Lett.* **41** 449
 - [33] Yuanjie L et al 2020 Demonstration of β -Ga₂O₃ junction barrier schottky diodes with a baliga's figure of merit of 0.85 GW/cm² or a 5A/700 V handling capabilities *IEEE Trans. Power Electron.* **36** 6179–82
 - [34] Gong H H, Chen X H, Xu Y, Ren -F-F, Gu S L and Ye J D 2020 A 1.86-kV double-layered NiO/ β -Ga₂O₃ vertical p-n heterojunction diode *Appl. Phys. Lett.* **117** 022104
 - [35] Sharma R, Xian M, Chaker Fares M E, Law M T, Hobart K D, Ren F and Pearton S J 2021 Effect of probe geometry during measurement of >100 A Ga₂O₃ vertical rectifiers *J. Vac. Sci. Technol. A* **39** 013406
 - [36] Wang B, Xiao M, Yan X, Wong H Y, Jiahui M, Sasaki K, Wang H and Zhang Y 2019 High-voltage vertical Ga₂O₃ power rectifiers operational at high temperatures up to 600 K *Appl. Phys. Lett.* **115** 263503
 - [37] Wenshen L, Nomoto K, Jena D and Xing H G 2020 Thermionic emission or tunneling? The universal transition electric field for ideal Schottky reverse leakage current: a case study in β -Ga₂O₃ *Appl. Phys. Lett.* **117** 222104
 - [38] Rafique S, Han L, Mou S and Zhao H 2017 Temperature and doping concentration dependence of the energy band gap in β -Ga₂O₃ thin films grown on sapphire *Opt. Mater. Express* **7** 3561
 - [39] Werner J H and Güttler H H 1993 Temperature dependence of Schottky barrier heights on silicon *J. Appl. Phys.* **73** 1315
 - [40] Luke A M, Lyle K J, Favela E V, Das K, Popp A, Galazka Z, Wagner G and Porter L M 2021 Effect of metal contacts on (100) β -Ga₂O₃ Schottky *J. Vac. Sci. Technol. A* **39** 033202
 - [41] Yang T-H, Houqiang F, Chen H, Huang X, Montes J, Baranowski I, Kai F and Zhao Y 2019 Temperature-dependent electrical properties of β -Ga₂O₃ Schottky barrier diodes on highly doped single-crystal substrates *J. Semicond.* **40** 012801
 - [42] Cheung S K and Cheung N W 1986 *Appl. Phys. Lett.* **49** 85
 - [43] Yadav M K, Mondal A, Sharma S K and Baga A 2021 Substrate orientation dependent current transport mechanisms in β -Ga₂O₃/Si based Schottky barrier diodes *J. Vac. Sci. Technol. A* **39** 033203
 - [44] Cao L, Wang J, Harden G, Hancheng Y, Stillwell R, Hoffman A J and Fay P 2018 Experimental characterization of impact ionization coefficients for electrons and holes in GaN grown on bulk GaN substrates *Appl. Phys. Lett.* **112** 262103
 - [45] Kizilyalli C, Edwards A P, Aktas O, Prunty T and Bour D 2015 Vertical power p-n diodes based on bulk GaN *IEEE Trans. Electron Devices* **62** 414
 - [46] Yakimov E B, Polyakov A Y, Smirnov N B, Shchemerov I V, Vergeles P S, Yakimov E E, Chernykh A V, Xian M, Ren F and Pearton S J 2020 Role of hole trapping by deep acceptors in electron beam induced current measurements in β -Ga₂O₃ vertical rectifiers *J. Phys. D: Appl. Phys.* **53** 495108
 - [47] Yakimov E B et al 2020 Photosensitivity of Ga₂O₃ Schottky diodes: effects of deep acceptor traps present before and after neutron irradiation *APL Mater.* **8** 111105
 - [48] Kaplar R, Slobodyan O, Flicker J, Dickerson J, Smith T, Binder A and Hollis M 2019 Analysis of the dependence of

- critical electric field on semiconductor bandgap presented at 236TH ECS Meeting (Atlanta, GA, 13–17 October)
- [49] Radhakrishnan R, Witt T and Woodin R 2014 Temperature dependence design of silicon carbide schottky diodes *2nd IEEE Workshop Wide Bandgap Power Devices Appl. WiPDA 2014* (IEEE) pp 151–4
- [50] Xiao M, Palacios T and Zhang Y 2019 Leakage and breakdown mechanisms of GaN vertical power FinFETs *Appl. Phys. Lett.* **114** 163503
- [51] Zhou C, Jiang Q, Huang S and Chen K J 2012 Vertical Leakage/Breakdown Mechanisms in AlGaIn/GaN on Si Devices *IEEE Electron Device Lett.* **33** 1132
- [52] Yoshizumi Y, Hashimoto S, Tanabe T and Kiyama M 2007 High breakdown-voltage pn-junction diodes on GaN substrates *J. Cryst. Growth* **298** 875
- [53] Wang Z, Chen X, Ren -F-F, Shulin G and Jiandong Y 2021 Deep-level defects in gallium oxide *J. Appl. Phys.* **54** 043002
- [54] Hou C, York K R, Makin R A, Durbin S M, Gazoni R M, Reeves R J and Allen M W 2020 High temperature (500 °C) operating limits of oxidized platinum group metal (PtO_x, IrO_x, PdO_x, RuO_x) Schottky contacts on β -Ga₂O₃ *Appl. Phys. Lett.* **117** 203502
- [55] Ahn S, Ren F, Yuan L, Pearton S J and Kuramata A 2017 Temperature-dependent characteristics of Ni/Au and Pt/Au Schottky diodes on β -Ga₂O₃ *ECS J. Solid State Sci. Technol.* **6** P68
- [56] Higashiwaki M, Konishi K, Sasaki K, Goto K, Nomura K, Thieu Q T and Togashi R 2016 Temperature-dependent capacitance-voltage and current-voltage characteristics of Pt/Ga₂O₃ (001) Schottky barrier diodes fabricated on n-Ga₂O₃ drift layers grown by halide vapor phase epitaxy *Appl. Phys. Lett.* **108** 133503